Science of the Total Environment 817 (2022) 153002

Contents lists available at ScienceDirect

Science of the Total Environment

journal homepage: www.elsevier.com/locate/scitotenv

COVID-19 lockdown effects on a coastal marine environment: Disentangling perception versus reality

Federica Braga [a], Daniele Ciani [b], Simone Colella [b], Emanuele Organelli [b], Jaime Pitarch [b], Vittorio E. Brando [b], Mariano Bresciani [c], Javier A. Concha [b], Claudia Giardino [c], Gian Marco Scarpa [a], Gianluca Volpe [b], Marie-Hélène Rio [d], Federico Falcini [b,*]

[a] Consiglio Nazionale delle Ricerche, Istituto di Scienze Marine (CNR-ISMAR), Venice, Italy
[b] Consiglio Nazionale delle Ricerche, Istituto di Scienze Marine (CNR-ISMAR), Rome, Italy
[c] Consiglio Nazionale delle Ricerche, Istituto per il Rilevamento Elettromagnetico dell'Ambiente (CNR-IREA), Milan, Italy
[d] European Space Agency, European Space Research Institute (ESA-ESRIN), Frascati, Italy

HIGHLIGHTS

- Satellite data diagnose inland and marine water quality during COVID-19 lockdown.
- Lockdown apparently results in very low Chl-a concentration in coastal waters.
- Seasonal-environmental conditions make hard to disentangle lockdown effects.
- Environmental (first-order) causes enhanced water quality during the lockdown.
- Riverine bio-optical spectra highlight (second-order) lockdown effect.

GRAPHICAL ABSTRACT

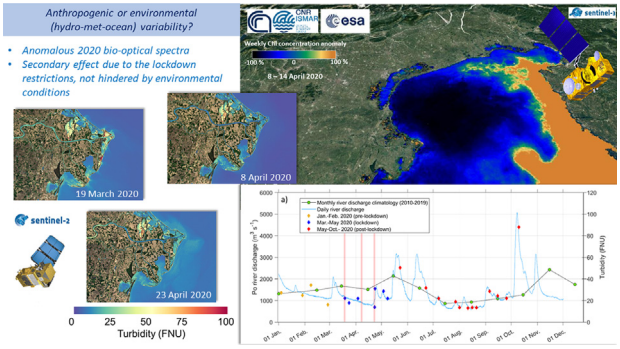

ARTICLE INFO

Article history:
Received 20 November 2021
Received in revised form 5 January 2022
Accepted 5 January 2022
Available online 11 January 2022

Editor: Martin Drews

Keywords:
COVID-19 lockdown
Coastal marine environment
Remote sensing
Inland-marine water connectivity

ABSTRACT

COVID-19 lockdown brought to a drastic reduction of anthropic impacts on the environment worldwide, including the marine-coastal system. Earth-Observation (EO) data have the potential to monitor and diagnose the effects of the lockdown in terms of water quality. Here we connect the dots among some coastal environmental changes that occurred during the Italian COVID-19 lockdown by using EO data, also seeking to assess connectivity between inland and marine systems. We present a holistic analysis of spatial and temporal variability of environmental parameters in the North Adriatic Sea, Mediterranean basin, exploiting the synergy of different satellite sensors, as well as hydrologic data from in situ observations. Our analysis indicates a favourable interplay of environmental variability that resulted in negative anomalies of Chlorophyll-a concentration, with respect to the climatologic values. Peculiar meteo-oceanographic and hydrological conditions made hard to disentangle potential anthropogenic effects. However, a multi-year hierarchical cluster analysis of riverine remote sensing reflectances groups together the optical properties of inland waters during the lockdown. This emergent cluster highlights the possibility of a second-order, anthropogenic effect that, superimposed to the (first-order) environmental natural causes, may have enhanced water quality during the lockdown.

* Corresponding author.
E-mail address: federico.falcini@cnr.it (F. Falcini).

http://dx.doi.org/10.1016/j.scitotenv.2022.153002

1. Introduction

Since 23 February 2020, a series of restrictions, including quarantine and social distancing, were enacted in Italy after the identification of two clusters of COVID-19 in its northern plain (Fig. 1). As of March 9th, widespread lockdown extended to the whole country (Lazzerini and Putoto, 2020; Harlan and Pitrelli, 2020; Di Donato et al., 2020), a fact that represented a unique, unplanned experiment of drastic reduction of anthropic impacts on the environment (e.g., traffic, touristic activities, and some non-primary industrial and agricultural activities; see race.esa.int), in particular, over regions of significant polluted inputs (Kalita and Talukdar, 2021).

In such a context, environmental scientists and the Earth-Observation (EO) community wondered about the real effects of the reduction of anthropogenic input in terms of water quality in coastal areas (Braga et al., 2020; Vijay Prakash et al., 2021). Coastal regions are, indeed, characterized by the presence of many industrialized or touristic areas and they were supposed to be one of the most crucial environments that might experience the effect of the 2020 lockdown. However, these areas are also strongly influenced by multiscale meteo-oceanographic and hydrological processes (Vermaat et al., 2008; Delhez and Barth, 2011; Devlin et al., 2015). Connections between natural environmental variability, anthropogenic forcing, and ecological response in these areas can occur across a large range of interacting spatial, temporal, and organizational scales; this makes monitoring activity a rather challenging task (Stock et al., 2011; Ostendorf, 2011; Dickey-Collas, 2014). Disentangling the mutual effect of anthropic pressures and environmental variability requires a multi-scale approach, i.e., the ability of detecting fast responses on a short time scale and monitoring local (i.e., small-scale) processes over large domains, based on consistent datasets that can assess statistically significant anomalies (Halpern et al., 2008; Zingone et al., 2010; Vermeulen et al., 2011). Satellite-based approaches proved to be the most suitable tools for this task (Harvey et al., 2015; Colella et al., 2016; Gohin et al., 2019).

Phytoplankton bloom occurrence is considered a direct proxy for coastal ecosystem health (Conley et al., 2009; Siegel et al., 2011; Blondeau-Patissier et al., 2014). Anthropogenic enrichment of the water column with nutrients can cause an increase in the biomass of phytoplankton, resulting in a range of undesirable disturbances in the marine ecosystem such as an increased turbidity, a decrease of biodiversity, deoxygenation, fish kills and aquatic vegetation loss (Gulati and van Donk, 2002). Satellite Ocean-Colour (OC) observations provide regular Chlorophyll-a (Chl-a) concentration observations at high spatial and temporal frequencies, using a harmonized methodology over large areas. The two replicates of the Copernicus Multi Spectral Instrument (MSI) optical sensor (Drusch et al., 2012), on board the Sentinel-2 satellites, helped monitoring the evolution of the Venice lagoon (Fig. 1) water transparency as well as of main European rivers largely affected by goods transportation, tourism, and agriculture (Braga et al., 2020; Zambrano-Monserrate et al., 2020; Yunus et al., 2020). On the other hand, the Ocean and Land Colour Instrument (OLCI) sensor (Donlon et al., 2012), on board the Sentinel-3 satellites, offers a time-series of OC observations at medium spatial resolution (300 m) with higher signal-to-noise ratio and higher temporal frequency, allowing for robust statistical analyses on coastal environments, eventually highlighting signals of human pressures on key hot spots.

By using both MSI and OLCI data, we focus on water quality changes occurred in the North Adriatic Sea (NAS; Mediterranean Sea; Fig. 1) and, in particular, off the Venice lagoon and the Po River Delta coastal area, where intense human activities (e.g., industry, aquaculture, tourism) take place. The NAS (Fig. 1) is a semi-enclosed basin, characterized by a large number of river inputs that act in a limited spatial extent (Cozzi and

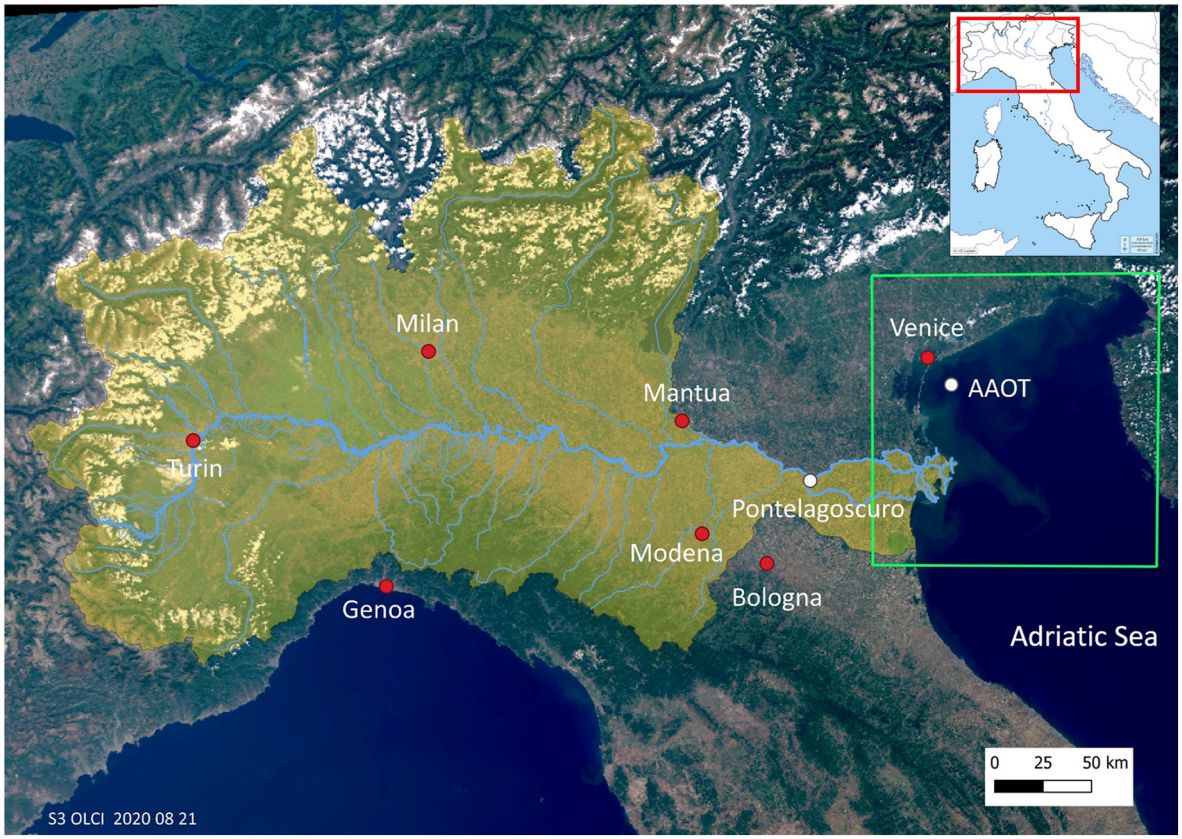

Fig. 1. OLCI image of the Po River drainage basin (Northern Italy). Red dots show the main cities within or adjacent to the drainage basin (yellow area). White dots show the location of Acqua Alta Oceanographic Platform (AAOT) station and Pontelagoscuro gauging station. Green square represents the area we investigated by the satellite-based analysis.

Giani, 2011; Brando et al., 2015). Along with the freshwater inputs, wind-driven forcing can influence the vertical and horizontal current fields, and, consequently, patterns of biogeochemical tracers in this region (Bignami et al., 2007). The Po River is the largest river of Italy and among the main rivers in the Mediterranean Sea in terms of water discharge, debouching in the NAS (Struglia et al., 2004) (Fig. 1). It flows through one of the most urbanized and productive (mainly agriculture and industry) regions of Europe and its discharge exhibits large inter-annual variability (Zanchettin et al., 2008).

Because of widespread of pandemic, since 9 March 2020, the whole region that encompasses the Po River basin and the Venice area experienced a major breakdown of its economy. In particular, the unprecedented water transparency in the Venice lagoon was widely covered by international news outlets and social media (www.nytimes.com/2020/07/02/travel/venice-coronavirus-tourism.html). Similar conditions were observed in the whole coastal region (Depellegrin et al., 2020) and, in general, in many other touristic and industrial hotspots in the whole country (abcnews.go.com/International/wireStory/italys-seas-speak-tourists-boats-cleaner-water-70966642).

Our goal is to assess the environmental effects of this unprecedented change of anthropic activities by providing evidence from EO and in situ data. Emergent patterns are investigated in the light of riverine bio-optical and hydrologic data, thus linking river runoffs, meteo-oceanographic conditions, water quality, and the potential reduction of anthropic inputs and stressors due to the lockdown.

2. Methods

2.1. Remote sensing data and processing

Weekly Chl-a concentrations rely on OLCI full resolution observations. We downloaded the full time series (May 2016–present) of OLCI Level-2 full resolution (300 m) data from the EUMETSAT data centre (eumetsat.int, coda.eumetsat.int and codarep.eumetsat.int). Data were then extracted and remapped over a regular equirectangular grid in the NAS. We applied the CMEMS operational algorithms for phytoplankton Chlorophyll retrieval (Volpe et al., 2019), adapted to OLCI bands (the algorithm exploits the 555 nm band, while OLCI has the band centred over the 560 nm channel) and implemented on a daily basis. Chl-a product is, therefore, the result of a weighted average between an algorithm for open waters (Case I) and another for coastal waters (Case II), in which the weighting factor is calculated for every pixel based on the similarity to the Case I and Case II end members. OLCI daily time series was then turned into a weekly time series by averaging on a pixel-by-pixel basis. OLCI revisit-time at the latitude of the Mediterranean Sea is roughly one day so that a weekly product was deemed of appropriate temporal resolution for allowing the target area to be sampled as completely and regularly as possible. For each pixel the average and standard deviation was computed from a data cube of 3 pixels × 3 pixels × 7 days. This averaging reduced random noise and alleviated the lack of data mostly due to clouds. To investigate the impact of the lockdown, all weekly data from 2016 to 2019 concurred to the generation of the weekly climatology, which was then used as reference for the analysis. Finally, we considered the difference between the 2020 weekly observations and the weekly climatologies. This difference was judged against the climatology in order to obtain a relative, dimensionless value.

MSI Level 1 Top-Of the Atmosphere radiances, with a spatial resolution of 10, 20, and 60 m, were downloaded from Copernicus Open Access Hub and atmospherically corrected with the ACOLITE software (Vanhellemont, 2019) in order to calculate spectra of remote sensing reflectances (R_{rs}) at Pontelagoscuro gauging station before, during, and after the lockdown. Spectral minimum of total absorption determines the peak at the Green band (560 nm) of the spectra is, usually, influenced by a minimum absorption of algal pigments and scattering by inorganic particles and phytoplankton (Stramski et al., 2004; Gitelson et al., 2008). The secondary peak at 704 nm is caused by a small window absorption between the second absorption peak of Chl-a at 665 nm (Gitelson et al., 2008) and the sharply increasing absorption of water molecules. This peak only becomes visible at significant Chl-a concentrations, mostly findable in coastal or inland waters (Gitelson, 1992, Gons et al., 2002, Dall'Olmo and Gitelson, 2005).

To detect the characteristic peaks in the spectral reflectance associated with significant Chl-a concentrations in turbid, productive waters, we calculated the Normalized Difference Chlorophyll Index (NDCI) (Mishra and Mishra, 2012) and adapted to MSI bands (Caballero et al., 2020):

$$NDCI = \frac{R_{rs}(704) - R_{rs}(665)}{R_{rs}(704) + R_{rs}(665)}. \quad (1)$$

Remote-sensing reflectances (R_{rs}) were also converted into Water Turbidity, expressed in formazin nephelometric unit [FNU] (Dogliotti et al., 2015) and into Chl-a concentration (in mg m^{-3}) (Pinardi et al., 2018). To assess the accuracy of turbidity products derived from MSI imagery, in situ data collected in the Venice lagoon was used. In particular, turbidity profiles were recorded during field activities from 2017 onwards with a SeaPoint turbidity meter (SeaPoint®). The correlation for 198 match-ups between satellite-derived estimates of turbidity versus in situ measurements was statistically significant with a coefficient of correlation r of 0.962, a coefficient of determination R^2 of 0.925, a RMSE of 2.44 FNU (Supplementary Fig. S1). These results are consistent with the accuracy assessed for ACOLITE-derived turbidity retrieved from Landsat-8 in the North Adriatic coastal waters (Braga et al., 2017). R_{rs}, Chl-a concentration, and Water Turbidity were extracted from a 5 × 5 pixels region of interest in the Po River, near Pontelagoscuro gauging station.

Satellite-based Sea-Surface Temperature (SST) was obtained from CMEMS (Product SST_MED_SST_L4_NRT_OBSERVATIONS_010_004), by a gap-free, optimally interpolated product and was built by using observations acquired from different platforms, e.g. Envisat, NOAA-18, MetOpA, Aqua, Terra, MetOpB, NPP, Meteosat11, as well as Sentinel 3A and Sentinel 3B satellites (Buongiorno Nardelli et al., 2013; Buongiorno Nardelli et al., 2015). The optimal interpolation procedure consists in the data extraction and quality control, the merging of the multi-platform observations and the interpolation on a regular 0.01° grid. The gap-free analysis processing is obtained via objective analysis (Le Traon, 1990) collecting SST observations free of diurnal warming effects (from 18:00 to 6:00 UTC) using spatial and temporal decorrelation lengths of 5 km and 1 day, respectively. This SST is thus representative of a foundation SST (i.e., temperature free of diurnal temperature variability) (Minnett et al., 2019).

2.2. In situ data

Data of hourly water discharge for the Po River at the Pontelagoscuro gauging station were obtained from the Environmental Protection Agency of the Region of Emilia Romagna (ARPA-ER). Sea temperature and wind direction and speed were measured at AAOT and are provided by the *Centro Previsione e Segnalazione Maree* of the city of Venice.

2.3. Marine currents

The Mediterranean Forecasting System is a hydrodynamic primitive equations model for the Mediterranean Basin (Clementi et al., 2019). The model outputs are distributed through the Copernicus Marine Environment Monitoring Service (CMEMS, Product MEDSEA-ANALYSIS- FORECAST-PHY-006-013) and provide daily to hourly fields of horizontal currents, temperature, salinity and free-surface elevation. The outputs are given on a 1/24° regular grid and 125 unequally spaced vertical levels. The core of the hydrodynamic model is the NEMO (Nucleus for European Modelling of the Ocean) model, the wave component is provided by Wave Watch-III. The numerical simulations assimilate satellite sea-surface temperature, altimeter-derived along-track sea-level anomalies and in situ measured salinity profiles.

2.4. Hierarchical cluster analysis

To classify the entire R_{rs} spectra acquired by Sentinel-2 at 9 bands in the range 443–865 nm into cluster trees (i.e., dendrograms), a hierarchical cluster analysis (HCA) was applied for the 2020 R_{rs} spectra (time constrained single-year) and for R_{rs} spectra collected from 2018 to 2020 (multi-year). The use of HCA has been widely stressed for application of remote sensing, using hyperspectral data, especially when coupled with the derivative spectra of R_{rs} (and its derived optical properties) that enhance the signature of absorbing material in water such as phytoplankton Chlorophyll and other pigments. The classification of spectra was performed by using linkage algorithms and similarity criteria (Torrecilla et al., 2011; Organelli et al., 2017). The high similarity we observed in this study was due to the analysis performed on ordinary spectra composed by only 9 bands. Briefly, the unweighted pair-group average linkage algorithm was used to group the spectra according to the average distance between all members. To better characterize the impact of lockdown phases on the Po River optical properties, the single-year HCA was constrained in time in order to compute the similarity between spectra acquired consecutively during 2020. The multi-year HCA was not time constrained, in order to highlight differences of the 2020 R_{rs} spectra with those collected during the other years. The similarity level between spectra was based on the cosine distance which returns values from 0 (i.e., no similarity) to 1 (i.e. the high similarity). Cluster analysis was carried out by the free statistical software PAST version 3.04.

Along with the single-year and multi-year HCA, we performed the analysis of variance (ANOVA) of Chl-a concentration, Water Turbidity, and Po River discharge, calculating the probability values for each single parameter. In particular, for each cluster of the two HCAs we calculated mean values, standard deviation, and probability values (p-value) of Chl-a concentration, Water Turbidity, and Po River discharge.

3. Results and discussions

3.1. Anomalies of OLCI-based Chlorophyll-a concentration

We calculated weekly deviations from climatology of Chl-a concentrations by using OLCI data over the NAS. In our study area, strongly influenced by river inputs and human activities, large values of Chl-a concentration result from the discharge of urban sewage, industrial runoffs, and fertilizers from agriculture activities over watersheds (Penna et al., 2004; Colella et al., 2016; Cozzi and Giani, 2011).

Starting from 18 March 2020 (i.e., about a week after the beginning of the Italian 2020 lockdown), the sequence of weekly mean and anomalies highlighted a general, decreasing trend of Chl-a concentration along the Italian coastal zone facing the NAS as well as off the whole Po River Delta (Fig. 2). In particular, around mid-April 2020, the weekly anomalies showed very low values (Fig. 2b, c, d), with negative, relative changes close to 100%.

Although such an intriguing pattern might be due to (or at least enhanced by) natural environmental conditions, such as moderate winds and riverine drought, it is worth investigating the striking coincidence between the consistent Chl-a concentration decrease, occurred form mid-March and the 2020 lockdown, in the light of variability of other natural phenomena. Indeed, while such a decrease of biomass was expected to occur in coastal areas (Braga et al., 2020; Zambrano-Monserrate et al., 2020; Yunus et al., 2020), offshore areas might not be directly affected by inputs of anthropogenic origin.

3.2. Meteo-oceanographic conditions

The negative anomalies of Chl-a concentration (Fig. 2) we found off the Venice Lagoon and the Po River Delta likely result from the cumulated

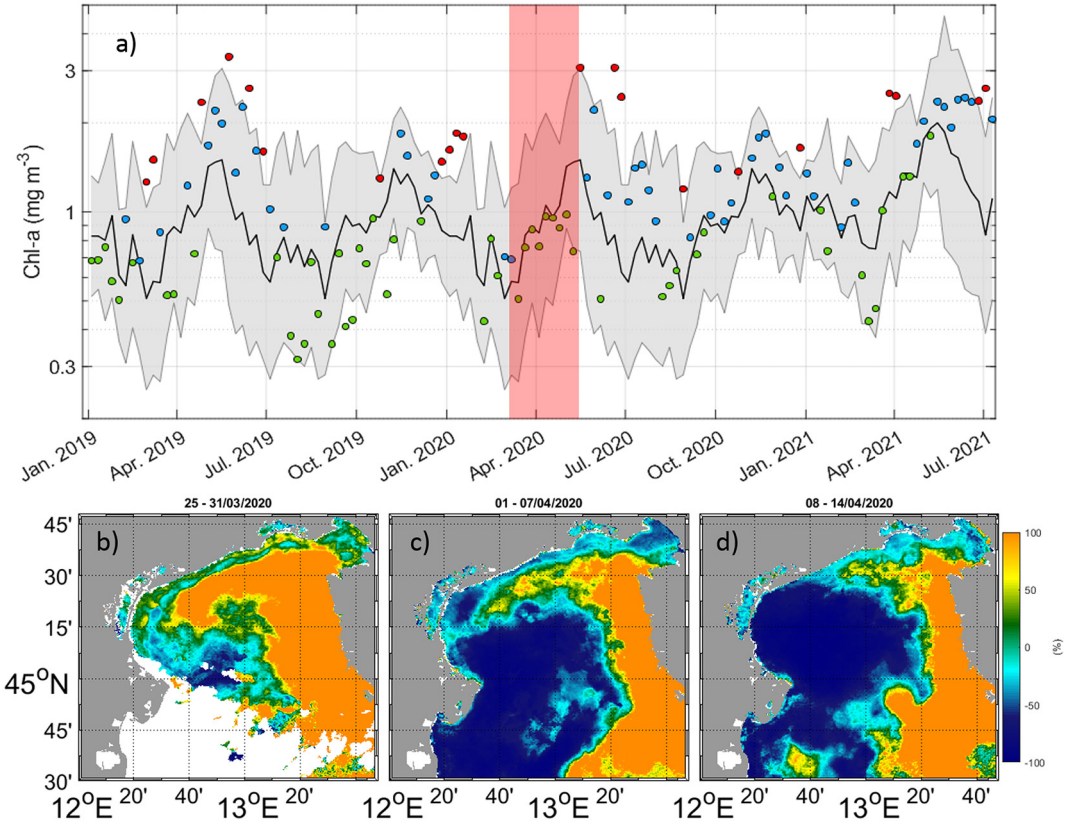

Fig. 2. (a) Chl-a concentration in the North Adriatic Sea during the Italian lockdown from OLCI (See Methods); the black line indicates the 2017–2019 climatologic values of Chl-a concentration; the grey shadow indicates the standard deviation; dots represent the weekly means of Chl-a concentration (green) below the climatologic value, (blue) above the climatologic value and below the standard deviation, (red) above the climatologic value and above the standard deviation; the red shaded area indicates the 2020 Italian lockdown. Anomalies of Chl-a concentration for the weeks (b) 25–31 March, (c) 1–7 April, and (d) 8–14 April 2020.

impact of a number of natural phenomena. Low wind magnitudes, recorded at the Acqua Alta Oceanographic Tower (AAOT) station (Fig. 1), from 5 to 20 April 2020, suggested the maintenance of vertical stratification of the water column (Fig. 3a, b), which may have hindered nutrient-rich waters due to mixing processes that would have enhanced the growth of phytoplankton. This hypothesis is confirmed by a significant increase of water temperature at the AAOT station during that period (Fig. 3a, b).

Satellite-derived Sea Surface Temperature (SST) at AAOT (Fig. 3b, validated with in situ measurements at AAOT) shows an increase, in particular, from 5 to 20 April 2020, likely due to the mild wind activity (Fig. 3b, c, d, e). This condition resulted in a weak alongshore transport of riverine nutrients from the northern sector of the basin (Fig. 3f, g, h). The warm river-plume bulge and the associated SST pattern along the north-west coast of the basin marked a reduction of the well-known cyclonic, cold coastal

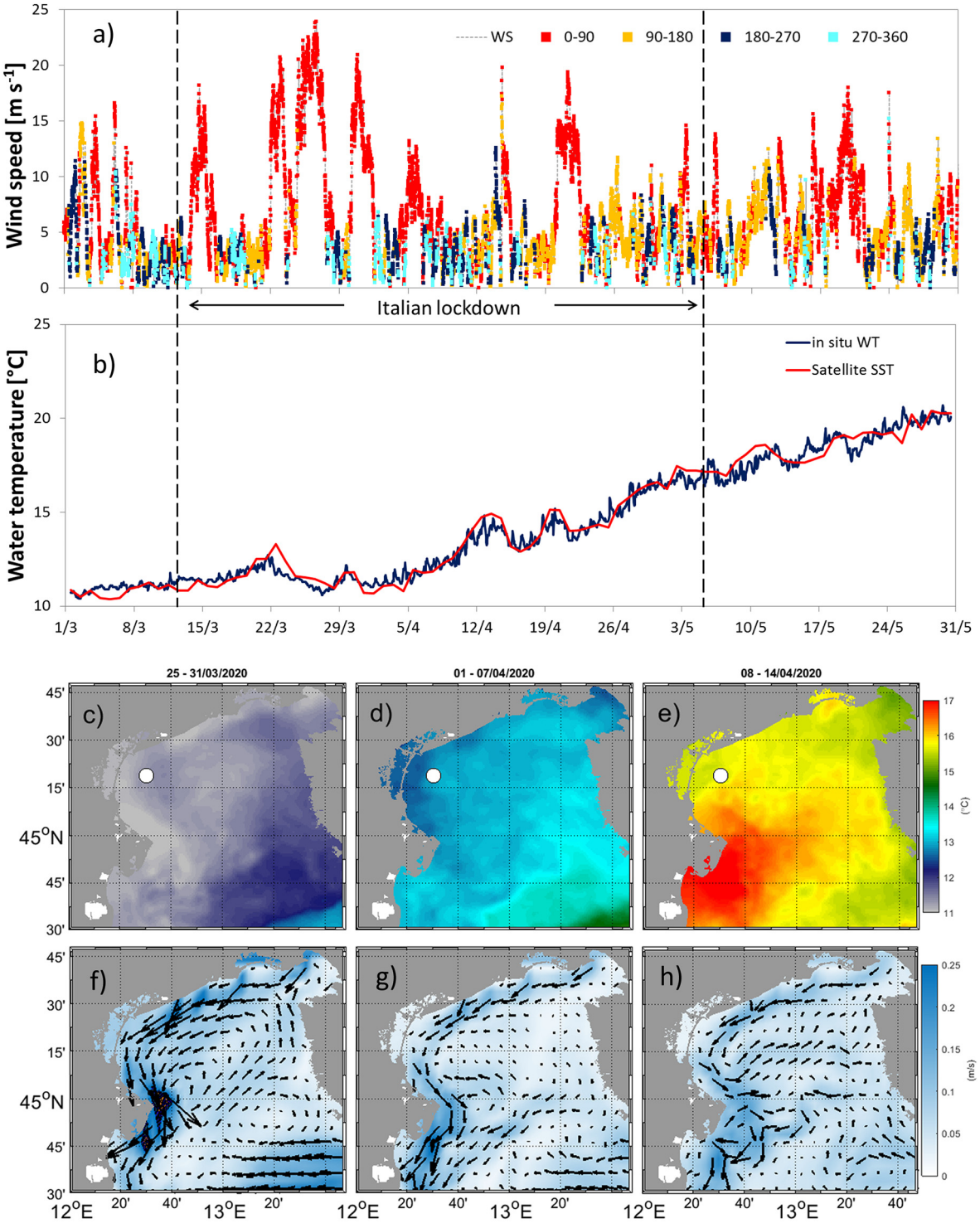

Fig. 3. Time series of (a) wind speed (WS) and direction measurements (red = 0°-90°, yellow = 90°-180°, blue = 180°-270°, cyan = 270°-360°) at the AAOT station and (b) water temperature (WT) at a depth of 2 m (blue line) and SST (red line), recorded at AAOT station from 1 March to 31 May 2020. Means of Sea Surface Temperature for the weeks (c) 25–31 March, (d) 1–7 April, and (e) 8–14 April 2020; the white dot indicates the location of the AAOT. Means of sea surface (1 m) marine currents for the weeks (f) 25–31 March, (g) 1–7 April, and (h) 8–14 April 2020.

current (Bignami et al., 2007; Nof and Pichevin, 2001) that constitutes the natural conveyor belt of the North Adriatic river-plumes, i.e., the primary source of nutrient and sediment loads that flow southward. This likely resulted to a mild riverine nutrient advection along the coastal area, which was further favoured by the absence of wind-induced mixing we recorded during that period (Fig. 3).

3.3. River inputs and MSI-derived Water Turbidity

Hydrological data of the Po River at Pontelagoscuro station (~90 km upstream the river mouth) showed that the lowest anomaly of Chl-a concentration off the Po River Delta (Fig. 2) occurred during a minimum stage of water discharge, recorded between 10 and 20 April 2020 (Fig. 4a). The low water discharge we observed (about 40% lower than the 2010–2019 climatological value) confirmed the mild advection of nutrients from the Po River tributaries, as well as the low input of cold riverine water we observed from SST imagery off the Po River delta (Fig. 3c, d, e).

Water Turbidity values, derived from MSI images near Pontelagoscuro gauging station, confirmed a general correlation between nutrient-poor river runoff and synchronous water discharge measurements (Fig. 4b, c, d, e). This correlation seems to be slightly affected by seasonal effects and results to be particularly evident after the lockdown. Before and during the lockdown, indeed, water discharge and turbidity show a weak correlation, likely due to threshold limitations on sediment supply and/or biogeochemical activity (Syvitski and Kettner, 2011; Tesi et al., 2013).

3.4. MSI-based spectral classification of the Po River runoff

To investigate the inland water bio-optical properties of the Po River and their eventual relationship with the biogeochemical pattern we

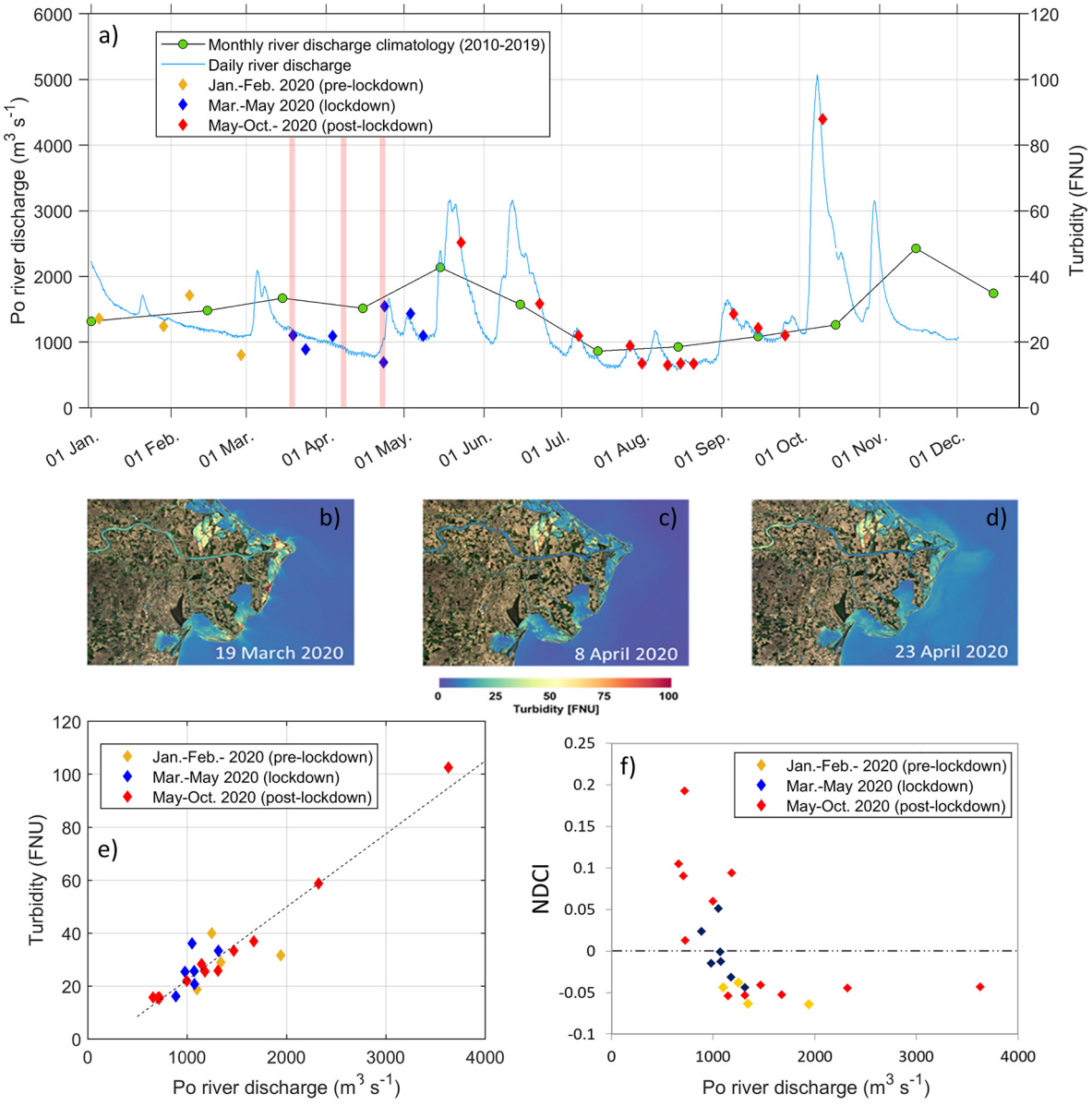

Fig. 4. (a) Daily river discharge measured at Pontelagoscuro gauging station compared with monthly climatology for the period 2010–2019. Diamonds represent average Water Turbidity values extracted from satellite maps near Pontelagoscuro station (lockdown period is marked in blue); the three vertical line indicate the Water Turbidity maps on (b) 19 March, (c) 8 April, and (d) 23 April 2020. (e) Scatter plot of the MSI-derived turbidity vs daily river discharge, measured at Pontelagoscuro gauging station. (f) Scatter plot of the spectral slope of MSI-derived R_{rs} between 665 nm and 704 nm (see Methods) versus daily discharge of Po River, recorded at Pontelagoscuro. NDCI was calculated with Eq. (1) (see Methods). Water turbidity was retrieved according to Dogliotti et al. (2015). Colours indicate the pre-lockdown (yellow), the lockdown (blue), and the post-lockdown (red) periods.

observed along the coastal areas, we analyzed MSI remote sensing Reflectance (R_{rs}) spectra, collected before, during, and after the 2020 lockdown, extracted at Pontelagoscuro gauging station (Supplementary Fig. S1).

MSI spectra showed that the R_{rs} peak magnitude in the NIR was often comparable to the green band (560 nm), indicating high Chl-a, while, for some dates, the NIR reflectance values were smaller than the R_{rs} in the red band (665 nm), due to low Chl-a concentration. In particular, four R_{rs} spectra in the pre-lockdown period (January–February 2020; Supplementary Fig. S1) showed similar characteristics in magnitude and shape as those of lockdown period (March–May 2020; Supplementary Fig. S1), except the two spectra with a reflectance peak in the NIR, due to high Chl-a concentration, occurred on 8 and 23 April 2020.

Spectra for the post-lockdown (Supplementary Fig. S1) exhibited highly variation in both magnitude and shape. A significant R_{rs} peak at 704 nm, respect to neighbouring bands is characteristic of high Chl-a concentrations, mostly findable in coastal or inland waters (Gitelson, 1992, Gons et al., 2002, Dall'Olmo and Gitelson, 2005). Here, this feature was quantified with the Normalized Difference Chlorophyll Index (NDCI; Fig. 4f). Positive NDCI values were observed at Po River discharges that were lower than 1000 $m^3\ s^{-1}$. Negative NDCI values were observed for higher discharges. This particular pattern clearly suggests the presence of a Chlorophyll-a absorption occurring during low discharge, while higher energetic river conditions seem to hinder phytoplankton growth (Pinder et al., 1997).

The Hierarchical Cluster Analysis (HCA) (Torrecilla et al., 2011; Uitz et al., 2015; Organelli et al., 2017) successfully grouped the 2020 MSI spectra into five major clusters that are not strictly correlated with the lockdown phases (Fig. 5a; Table 1).

Among the five groups identified by HCA, the first cluster included only spectra corresponding to the pre-lockdown period. The spectra we observed during the lockdown were instead grouped into two different clusters, and the second one showed high similarity with spectra from 23 May to 27 July 2020, which corresponded to the post-lockdown phase. The remaining spectra, acquired during post-lockdown in August, September, and October 2020, were contained in the fourth and fifth clusters (Fig. 5a; Table 1). Thus, the stop of the human activities due to the COVID-19 pandemic was not sufficient to significantly affect the optical properties of the Po River. This suggests that the spectral variability of R_{rs} was driven, at first order, by natural phenomena.

The five clusters of 2020 MSI R_{rs} spectra identified by HCA resulted from the seasonal variability of Chl-a concentration, water turbidity and discharge, observed for the Po River (Fig. 5b; Table 1). The spectra from the first, and pre-lockdown cluster were acquired when the river discharge was decreasing and the Water Turbidity was still high (>20 FNU). The interplay between low Chl-a concentrations in the river, low turbidity (<30 FNU), and low discharge (about 1000 $m^3\ s^{-1}$) resulted in the second cluster of spectra collected during the lockdown between 19 March and 8 April 2020. Differently, the spectral features of R_{rs} in the third cluster responded to a new increase of the Po River discharge (up to 2500 $m^3\ s^{-1}$) and thus of the water turbidity due to snow melting from the Alps and the Apennines (Zanchettin et al., 2008; Grilli et al., 2020). In August 2020, when the impact of water coming from surrounding mountains was low (i.e., riverine discharges < 1000 $m^3\ s^{-1}$), high Chl-a concentrations (up to 60 mg m^{-3}) determined the R_{rs} spectral optical properties grouped within the fourth cluster (Fig. 5a, b; Table 1). A new increase in water turbidity and discharge differentiated further the R_{rs} spectral properties from September and

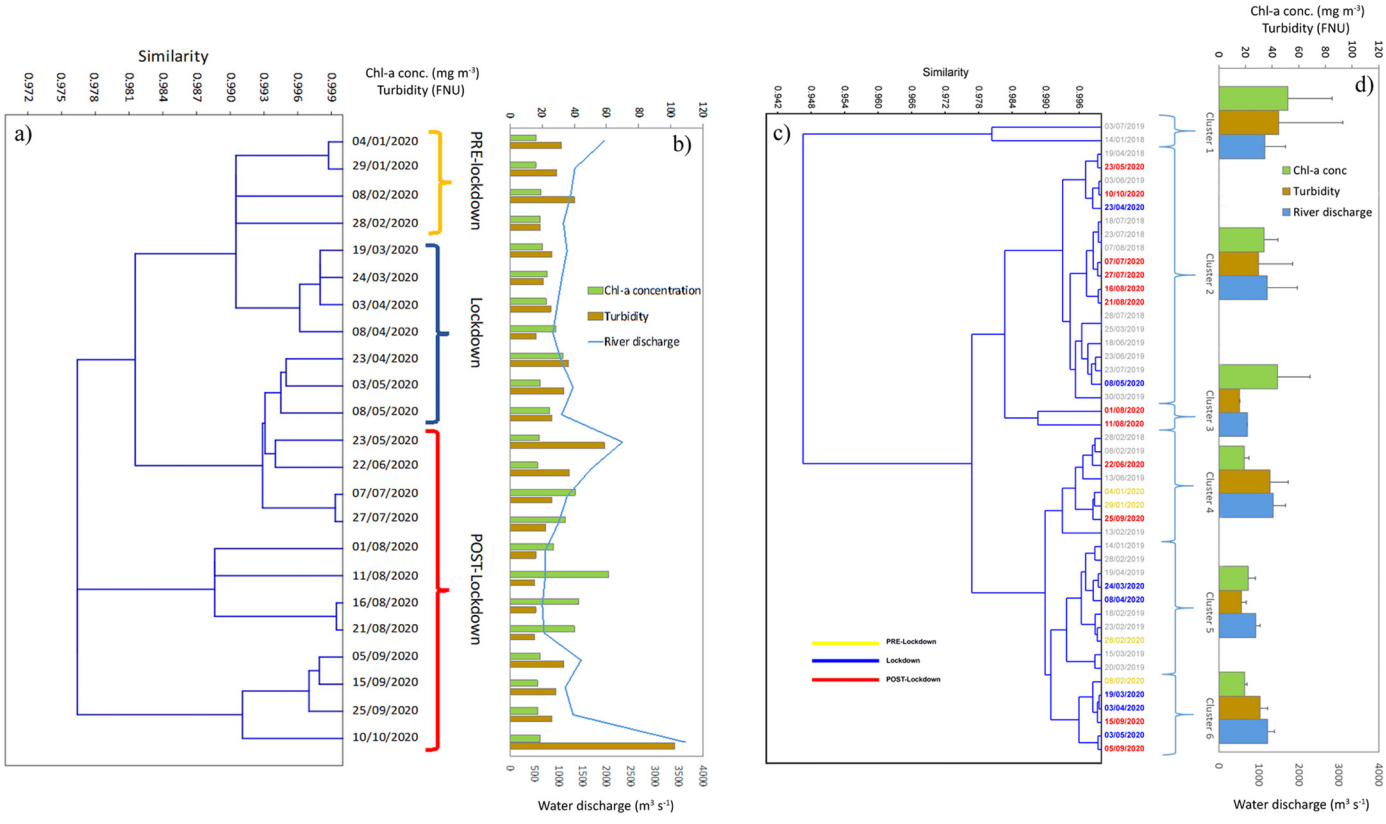

Fig. 5. a) Results of the HCA performed on MSI R_{rs} spectra between 443 and 865 nm, extracted from the Po river channel near Pontelagoscuro gauging station for the periods before, during and after the lockdown. b) Chlorophyll concentration, Water Turbidity (derived from MSI), and Po River discharge near the Pontelagoscuro gauging station corresponding to the date of acquisition of the Sentinel2 R_{rs} spectra. Data are shown in chronological order. c) Results of the multi-year HCA performed on MSI R_{rs} spectra between 443 and 865 nm, extracted from the Po River channel at Pontelagoscuro gauging station from 2018 to 2020. d) Means (and standard deviation) of Chl-a concentration, Water Turbidity (derived from MSI), and Po River discharge near the Pontelagoscuro gauging station corresponding to each cluster, identified by the HCA.

Table 1
Mean values and standard deviations (σ) of Chl-a concentration, Water Turbidity, and Po River water discharge related to the cluster we identified in both single-year (2020) and multi-year (2018–2020) HCA. The table shows the probability value (p-value) obtained from the ANOVA; Geen (yellow) shading indicates that the ANOVA p-value is less (greater) than the significant level of 0.05. Both p-values of the single- and multi-year analysis show that Chl-a concentration changes are statistically significant.

Single-year (2020) analysis of variance			
	Chl-a ± σ (mg m^{-3})	Turbidity ± σ (FNU)	Discharge ± σ (m^3 s^{-1})
Cluster 1	17.23 ± 1.83	29.86 ± 8.74	1406.07 ± 369.74
Cluster 2	23.50 ± 3.57	21.99 ± 4.53	1029.11 ± 125.21
Cluster 3	26.68 ± 9.43	34.04 ± 12.30	1372.06 ± 477.32
Cluster 4	42.68 ± 14.22	15.56 ± 0.26	700.60 ± 29.59
Cluster 5	17.84 ± 0.94	47.51 ± 36.87	1886.98 ± 1167.19
p-Value	0.002	0.120	0.080
Multi-year (2018–2020) analysis of variance			
	Chl-a ± σ (mg m^{-3})	Turbidity ± σ (FNU)	Discharge ± σ (m^3 s^{-1})
Cluster 1	51.73 ± 33.27	44.84 ± 48.06	1149.93 ± 523.29
Cluster 2	34.04 ± 10.20	29.65 ± 25.68	1211.99 ± 757.50
Cluster 3	44.03 ± 24.41	15.48 ± 0.40	719.49 ± 2.72
Cluster 4	19.09 ± 3.54	38.45 ± 13.71	1359.50 ± 307.50
Cluster 5	22.09 ± 5.19	17.09 ± 3.40	926.32 ± 109.40
Cluster 6	19.33 ± 1.87	31.03 ± 5.63	1221.40 ± 165.53
p-Value	0.00003	0.18828	0.46302

October 2020 (i.e. the fifth cluster) as a consequence of the heavy precipitations that characterize the northern part of Italy (Grilli et al., 2020).

From this analysis, we thus observed that the optical characteristics of the Po River in 2020 followed the natural variability of such riverine system, with no significant evidence of the lockdown (Fig. 5a, b). The resulting high-level riverine water quality was primary due to seasonal and hydrological conditions. However, we also notice from the analysis of variance (ANOVA) that, among the 2020 clusters, the Chl-a concentration is the sole parameter that shows statistically significant differences in its variability (Table 1). We therefore hypothesize that changes of Chl-a concentration might not strictly connected to the sole Po River discharge and Water Turbidity changes. This suggests the hypothesis of a second-order, non-seasonal, effect that slightly enhanced the good water quality we observed during the 2020 lockdown.

Accordingly, a multi-year HCA and the related ANOVA, conducted on MSI R_{rs} spectra from 2018 to 2020 at Pontelagoscuro gauging station, seems to highlight a cluster, i.e., Cluster 6 in Fig. 5c, d, that reinforce the hypothesis of an anomalous behaviour of Chl-a concentration during spring 2020 (Fig. 5c; Table 1). Indeed, Cluster 6 is identified by only R_{rs} spectra 2020, among which three of them are from spring 2020 spectra. Whereas, pre- and post-lockdown spectra from the year 2020 were well grouped with those of the other years and likely mark the seasonal runoff of the Po River. Chl-a concentration of Cluster 6 is particularly low and the ANOVA confirms that difference in Chl-a concentrations among clusters is statistically significant (Table 1). In particular, the probability value of mean Chl-a concentration of Cluster 6, when compared with Cluster 1-to-5 (all grouped together) is ~0.06, i.e., a value that mark the anomaly of this 2020 cluster in terms of Chl- concentration, with respect to the other clusters.

4. Conclusions

During the lockdown, significant negative anomalies of weekly Chl-a concentration were observed over a large part of the coastal, western sector North Adriatic basin. The particular combination of meteo-oceanographic and hydrological conditions was able to explain the negative anomalies of Chl-a concentration offshore the Venice lagoon and off the Po River delta. The mutual effect of environmental parameters, such as near surface winds and river discharge that caused well-stratified thermohaline conditions and a negligible runoff of nutrient inputs, maintained values of Chl-a concentration fairy low during the lockdown. Moreover, a Hierarchical Cluster Analysis, along with an analysis of variance, suggested that the variability of Chl-a concentration we observe from winter to fall 2020 is in accordance with a seasonal cycle.

Said that, we could not exclude a second order effect due to the decrease of human activities. It was, indeed, reasonable to hypothesize that the favourable environmental conditions we assessed did not hinder the effect of a reduction of anthropogenic inputs. The multi-year Hierarchical Cluster Analysis showed that the most of the spring 2020 R_{rs} spectra (i.e., those that correspond to the 2020 lockdown) tended to group in a specific cluster and, compared with other clusters that range from 2018 to 2020, this cluster showed a statistically significant difference in Chl-a concentration. In other words, such an intriguing, low value of Chl-a concentration we observed in both inland and marine waters during the 2020 lockdown, although mostly explained by seasonal variability of meteo-oceanographic conditions, statistically suggested a secondary, likely anthropogenic effect due to the lockdown restrictions, when analyzed in the frame of multi-year remote sensing and in situ data.

We finally remark that coastal dynamics of river plumes that show a significant reduction of nutrient loads of anthropogenic origin may be at the base of connectivity between inland and offshore water biogeochemical conditions. To test this hypothesis, it will be crucial the ad hoc synergy of additional satellite imagery for inland waters, including hyperspectral products, and in situ measurements of chemical/pollutant components.

Funding

This work was primarily supported by SOON (Satellite Observations for inland and cOastal water quality during COVID lock-dowN) project, funded by the European Space Agency via the contract Grant No. 578 4000128147/19/I-DT, by SNAPSHOT (Synoptic Assessment of Human Pressures on key Mediterranean Hot Spots) project, funded by the Department of Earth System Sciences and Environmental of CNR, and by the European Union's Horizon 2020 - Research and Innovation Framework Programme (CERTO Project, grant agreement no. 870349).

CRediT authorship contribution statement

FF and MHR, delineated and supervised the study. FB, DC, SC, EO, JP, VEB, MB, JC, CG, GMS, and GV collected, processed, and analyzed the

remote sensing and in situ data. FB, DC, EO, JP, MHR, and FF contributed with resources, analyzed the data and wrote the manuscript.

Declaration of competing interest

The authors declare that the research was conducted in the absence of any commercial or financial relationships that could be construed as a potential conflict of interest.

Acknowledgments

We thank Maurizio Ribera D'Alcalà, Mario Sprovieri, and Chiara Santinelli for the insightful discussion at the initial stage of the investigation.

Appendix A. Supplementary data

Supplementary data to this article can be found online at https://doi.org/10.1016/j.scitotenv.2022.153002.

References

Bignami, F., Sciarra, R., Carniel, S., Santoleri, R., 2007. Variability of Adriatic Sea coastal turbid waters from SeaWiFS imagery. J. Geophys. Res. Oceans 112 (C3).

Blondeau-Patissier, D., Schroeder, T., Brando, V.E., Maier, S.W., Dekker, A.G., Phinn, S., 2014. ESA-MERIS 10-year mission reveals contrasting phytoplankton bloom dynamics in two tropical regions of northern Australia. Remote Sens. 6 (4), 2963–2988.

Braga, F., Zaggia, L., Bellafiore, D., Bresciani, M., Giardino, C., Lorenzetti, G., Brando, V.E., 2017. Mapping turbidity patterns in the Po river prodelta using multi-temporal landsat 8 imagery. Estuar. Coast. Shelf Sci. 198, 555–567.

Braga, F., Scarpa, G.M., Brando, V.E., Manfe, G., Zaggia, L., 2020. COVID-19 lockdown measures reveal human impact on water transparency in the Venice lagoon. Sci. Total Environ. 736, 139612.

Brando, V.E., Braga, F., Zaggia, L., Giardino, C., Bresciani, M., Matta, E., Carniel, S., 2015. High-resolution satellite turbidity and sea surface temperature observations of river plume interactions during a significant flood event. Ocean Sci. 11 (6), 909–920.

Buongiorno Nardelli, B., Tronconi, C., Pisano, A., Santoleri, R., 2013. High and ultra-high resolution processing of satellite sea surface temperature data over southern european seas in the framework of MyOcean project. Remote Sens. Environ. 129, 1–16.

Buongiorno Nardelli, B., Pisano, A., Tronconi, C., Santoleri, R., 2015. Evaluation of different covariance models for the operational interpolation of high resolution satellite sea surface temperature data over the Mediterranean Sea. Remote Sens. Environ. 164, 334–343.

Caballero, I., Fernández, R., Escalante, O.M., Mamán, L., Navarro, G., 2020. New capabilities of sentinel-2A/B satellites combined with in situ data for monitoring small harmful algal blooms in complex coastal waters. Sci. Rep. 10 (1), 1–14.

Clementi, E., Pistoia, J., Delrosso, D., Escudier, R., Drudi, M., Grandi, A., Coppini, G., 2019. The Mediterranean analysis and forecasting physical system for the Copernicus Marine Service: description and skill assessment. MayGODAE OceanView Symposium 2019-OceanPredict19.

Colella, S., Falcini, F., Rinaldi, E., Sammartino, M., Santoleri, R., 2016. Mediterranean Ocean colour chlorophyll trends. PloS one 11 (6), e0155756.

Conley, D.J., Paerl, H.W., Howarth, R.W., Boesch, D.F., Seitzinger, S.P., Havens, K.E., Likens, G.E., 2009. Controlling eutrophication: nitrogen and phosphorus. Science 323 (5917), 1014–1015.

Cozzi, S., Giani, M., 2011. River water and nutrient discharges in the northern Adriatic Sea: current importance and long term changes. Cont. Shelf Res. 31 (18), 1881–1893.

Dall'Olmo, G., Gitelson, A.A., 2005. Effect of bio-optical parameter variability on the remote estimation of chlorophyll-a concentration in turbid productive waters: experimental results. Appl. Opt. 44 (3), 412–422.

Delhez, E., Barth, A., 2011. Science based management of coastal waters. J. Mar. Syst. 88 (1).

Depellegrin, D., Bastianini, M., Fadini, A., Menegon, S., 2020. The effects of COVID-19 induced lockdown measures on maritime settings of a coastal region. Sci. Total Environ. 740, 140123.

Devlin, M.J., Petus, C., Da Silva, E., Tracey, D., Wolff, N.H., Waterhouse, J., Brodie, J., 2015. Water quality and river plume monitoring in the great barrier reef: an overview of methods based on ocean colour satellite data. Remote Sens. 7 (10), 12909–12941.

Dickey-Collas, M., 2014. Why the complex nature of integrated ecosystem assessments requires a flexible and adaptive approach. ICES J. Mar. Sci. 71 (5), 1174–1182.

Di Donato, V., Reynolds, E., Picheta, R., 2020. All of Italy is in lockdown as coronavirus cases rise. https://edition.cnn.com/2020/03/09/europe/coronavirus-italy-lockdown-intl/index.html Accessed 4th May 2021.

Dogliotti, A.I., Ruddick, K.G., Nechad, B., Doxaran, D., Knaeps, E., 2015. A single algorithm to retrieve turbidity from remotely-sensed data in all coastal and estuarine waters. Remote Sens. Environ. 156, 157–168.

Donlon, C., Berruti, B., Buongiorno, A., Ferreira, M.H., F´em´enias, P., Frerick, J., Goryl, P., Klein, U., Laur, H., Mavrocordatos, C., Nieke, J., Rebhan, H., Seitz, B., Stroede, J., Sciarra, R., 2012. The global monitoring for environment and security (GMES) Sentinel-3 mission. Remote Sens. Environ. 120, 37–57.

Drusch, M., Del Bello, U., Carlier, S., Colin, O., Fernandez, V., Gascon, F., Hoersch, B., Isola, C., Laberinti, P., Martimort, P., Meygret, A., Spoto, F., Sy, O., Marchese, F., Bargellini, P., 2012. Sentinel-2: ESA's optical high-resolution mission for GMES operational services. Remote Sens. Environ. 120, 25–36.

Gitelson, A., 1992. The peak near 700 nm on radiance spectra of algae and water: relationships of its magnitude and position with chlorophyll concentration. Int. J. Remote Sens. 13 (17), 3367–3373.

Gitelson, A.A., Dall'Olmo, G., Moses, W., Rundquist, D.C., Barrow, T., Fisher, T.R., Holz, J., 2008. A simple semi-analytical model for remote estimation of chlorophyll-a in turbid waters: validation. Remote Sens. Environ. 112 (9), 3582–3593.

Gohin, F., Van der Zande, D., Tilstone, G., Eleveld, M.A., Lefebvre, A., Andrieux-Loyer, F., Saulquin, B., 2019. Twenty years of satellite and in situ observations of surface chlorophyll-a from the northern Bay of Biscay to the eastern English Channel. Is the water quality improving? Remote Sens. Environ. 233, 111343.

Gons, H.J., Rijkeboer, M., Ruddick, K.G., 2002. A chlorophyll-retrieval algorithm for satellite imagery (Medium resolution imaging Spectrometer) of inland and coastal waters. J. Plankton Res. 24 (9), 947–951.

Grilli, F., Accoroni, S., Acri, F., Bernardi Aubry, F., Bergami, C., Cabrini, M., Cozzi, S., 2020. Seasonal and interannual trends of oceanographic parameters over 40 years in the northern Adriatic Sea in relation to nutrient loadings using the EMODnet chemistry data portal. Water 12 (8), 2280.

Gulati, R.D., van Donk, E., 2002. Lakes in the Netherlands, their origin, eutrophication and restoration: state-of-the-art review. In: Nienhuis, P.H., Gulati, R.D. (Eds.), Ecological Restoration of Aquatic and Semi-Aquatic Ecosystems in the Netherlands (NW Europe). Developments in Hydrobiology. vol 166. Springer, Dordrecht. https://doi.org/10.1007/978-94-017-1335-1_5.

Halpern, B.S., Walbridge, S., Selkoe, K.A., Kappel, C.V., Micheli, F., D'Agrosa, C., Fujita, R., 2008. A global map of human impact on marine ecosystems. Science 319 (5865), 948–952.

Harlan, C., Pitrelli, S., 2020. Italy's coronavirus lockdown upends the most basic routines and joys. https://www.washingtonpost.com/world/italy-coronavirus-lockdown/2020/03/10/f7ed95c4-5ff6-11ea-ac50-18701e14e06d_story.html Accessed 4th May 2021.

Harvey, E.T., Kratzer, S., Philipson, P., 2015. Satellite-based water quality monitoring for improved spatial and temporal retrieval of chlorophyll-a in coastal waters. Remote Sens. Environ. 158, 417–430.

Kalita, S., Talukdar, H., 2021. COVID-19 Pandemic: An Unprecedented Blessing for Nature. The Impact of the COVID-19 Pandemic on Green Societies. 349.

Lazzerini, M., Putoto, G., 2020. COVID-19 in Italy: momentous decisions and many uncertainties. Lancet Glob. Health 8 (5), e641–e642.

Le Traon, P.Y., 1990. A method for optimal analysis of fields with spatially variable mean. J. Geophys. Res. Oceans 95 (C8), 13543–13547.

Minnett, P.J., Alvera-Azcárate, A., Chin, T.M., Corlett, G.K., Gentemann, C.L., Karagali, I., Vazquez-Cuervo, J., 2019. Half a century of satellite remote sensing of sea-surface temperature. Remote Sens. Environ. 233, 111366.

Mishra, S., Mishra, D.R., 2012. Normalized difference chlorophyll index: a novel model for remote estimation of chlorophyll-a concentration in turbid productive waters. Remote Sens. Environ. 117, 394–406.

Nof, D., Pichevin, T., 2001. The ballooning of outflows. J. Phys. Oceanogr. 31 (10), 3045–3058.

Organelli, E., Nuccio, C., Lazzara, L., Uitz, J., Bricaud, A., Massi, L., 2017. On the discrimination of multiple phytoplankton groups from light absorption spectra of assemblages with mixed taxonomic composition and variable light conditions. Appl. Opt. 56 (14), 3952–3968.

Ostendorf, B., 2011. Overview: spatial information and indicators for sustainable management of natural resources. Ecol. Indic. 11 (1), 97–102.

Penna, N., Capellacci, S., Ricci, F., 2004. The influence of the Po River discharge on phytoplankton bloom dynamics along the coastline of Pesaro (Italy) in the Adriatic Sea. Mar. Pollut. Bull. 48 (3–4), 321–326.

Pinardi, M., Bresciani, M., Villa, P., Cazzaniga, I., Laini, A., Tóth, V., Giardino, C., 2018. Spatial and temporal dynamics of primary producers in shallow lakes as seen from space: intra-annual observations from sentinel-2A. Limnologica 72, 32–43.

Pinder, L.C.V., Marker, A.F.H., Pinder, A.C., Ingram, J.K.G., Leach, D.V., Collett, G.D., 1997. Concentrations of suspended chlorophyll a in the humber rivers. Sci. Total Environ. 194, 373–378.

Siegel, D.A., Antoine, D., Behrenfeld, M.J., Fanton d'Andon, O.H., Fields, E., Franz, B.A., Goryl, P., Maritorena, S., McClain, C.R., Wang, M., 2011. Global ocean phytoplankton. State of the Climate in 2010, Bulletin of the American Meteorological Society. 93. AMS, Boston, MA, USA pp. S107–S110.

Stock, C.A., Alexander, M.A., Bond, N.A., Brander, K.M., Cheung, W.W., Curchitser, E.N., Werner, F.E., 2011. On the use of IPCC-class models to assess the impact of climate on living marine resources. Prog. Oceanogr. 88 (1–4), 1–27.

Stramski, D., Boss, E., Bogucki, D., Voss, K.J., 2004. The role of seawater constituents in light backscattering in the ocean. Prog. Oceanogr. 61 (1), 27–56.

Struglia, M.V., Mariotti, A., Filograsso, A., 2004. River discharge into the Mediterranean Sea: climatology and aspects of the observed variability. Retrieved Jul 8, 2021, fromJ. Clim. 17 (24), 4740–4751.. https.

Syvitski, J.P., Kettner, A., 2011. Sediment flux and the anthropocene. Philos. Trans. R. Soc. A Math. Phys. Eng. Sci. 369 (1938), 957–975.

Tesi, T., Miserocchi, S., Acri, F., Langone, L., Boldrin, A., Hatten, J.A., Albertazzi, S., 2013. Flood-driven transport of sediment, particulate organic matter, and nutrients from the Po River watershed to the Mediterranean Sea. J. Hydrol. 498, 144–152.

Torrecilla, E., Stramski, D., Reynolds, R.A., Millan-Nunez, E., Piera, J., 2011. Cluster analysis of hyperspectral optical data for discriminating phytoplankton pigment assemblages in the open ocean. Remote Sens. Environ. 115, 2578–2593.

Uitz, J., Stramski, D., Reynolds, R.A., Dubranna, J., 2015. Assessing phytoplankton community composition from hyperspectral measurements of phytoplankton absorption coefficient and remote-sensing reflectance in open-ocean environments. Remote Sens. Environ. 171, 58–74.

Vanhellemont, Q., 2019. Adaptation of the dark spectrum fitting atmospheric correction for aquatic applications of the landsat and Sentinel-2 archives. Remote Sens. Environ. 225, 175–192.

Vijay Prakash, K., Vimala, G., Preethi Latha, T., Jayaram, C., Nagamani, P.V., Laxmi, C.N., 2021. Assessment of water quality along the southeast coast of India during COVID-19 lockdown. Front. Mar. Sci. 8, 338.

Volpe, G., Colella, S., Brando, V.E., Forneris, V., La Padula, F., Di Cicco, A., Santoleri, R., 2019. Mediterranean Ocean colour level 3 operational multi-sensor processing. Ocean Sci. 15 (1), 127–146.

Vermaat, J.E., McQuatters-Gollop, A., Eleveld, M.A., Gilbert, A.J., 2008. Past, present and future nutrient loads of the North Sea: causes and consequences. Estuar. Coast. Shelf Sci. 80 (1), 53–59.

Vermeulen, S., Sturaro, N., Gobert, S., Bouquegneau, J.M., Lepoint, G., 2011. Potential early indicators of anthropogenically derived nutrients: a multiscale stable isotope analysis. Mar. Ecol. Prog. Ser. 422, 9–22.

Yunus, A.P., Masago, Y., Hijioka, Y., 2020. COVID-19 and surface water quality: improved lake water quality during the lockdown. Sci. Total Environ. 731, 139012.

Zambrano-Monserrate, M.A., Ruano, M.A., Sanchez-Alcalde, L., 2020. Indirect effects of COVID-19 on the environment. Sci. Total Environ. 728, 138813.

Zanchettin, D., Traverso, P., Tomasino, M., 2008. Po River discharges: a preliminary analysis of a 200-year time series. Clim. Chang. 89 (3), 411–433.

Zingone, A., Phlips, E.J., Harrison, P.J., 2010. Multi-scale variability of twenty-two coastal phytoplankton time series: a global scale comparison. Estuar. Coasts 33, 224–229. https://doi.org/10.1007/s12237-009-9261-x.